Capillary interactions in Pickering emulsions

J. Guzowski,[1] M. Tasinkevych,[2,3] and S. Dietrich[2,3]
[1]*Institute of Physical Chemistry, Polish Academy of Sciences, ul. Kasprzaka 44/52, PL-01-224 Warsaw, Poland*
[2]*Max-Planck-Institut für Intelligente Systeme, Heisenbergstrasse 3, D-70569 Stuttgart, Germany*
[3]*Institut für Theoretische und Angewandte Physik, Universität Stuttgart, Pfaffenwaldring 57, D-70569 Stuttgart, Germany*
(Received 24 March 2011; revised manuscript received 19 June 2011; published 1 September 2011)

The effective capillary interaction potentials for small colloidal particles trapped at the surface of liquid droplets are calculated analytically. Pair potentials between capillary monopoles and dipoles, corresponding to particles floating on a droplet with a fixed center of mass and subjected to external forces and torques, respectively, exhibit a repulsion at large angular separations and an attraction at smaller separations, with the latter resembling the typical behavior for flat interfaces. This change of character is not observed for quadrupoles, corresponding to free particles on a mechanically isolated droplet. The analytical results are compared with the numerical minimization of the surface free energy of the droplet in the presence of spherical or ellipsoidal particles.

DOI: 10.1103/PhysRevE.84.031401 PACS number(s): 83.80.Iz, 68.03.Cd, 83.80.Hj

I. INTRODUCTION

If colloidal particles get trapped at fluid-fluid interfaces they interact effectively via deformations of the interface. These so-called capillary interactions can easily be tuned by changing external fields and they depend sensitively on the shape of the particles. This makes them good candidates for designing self-assembling systems and provides a convenient experimental playground for studying basic issues of statistical mechanics in two dimensions in the presence of long-ranged interactions [1,2]. On the other hand, recent experiments [3] show that capillary forces between elongated particles floating on spherical interfaces can have important consequences for stabilizing so-called Pickering emulsions, which are formed by particle-covered droplets (e.g., oil) in a solvent (e.g., water).

Whereas considerable theoretical progress has been made in understanding capillary interactions at flat interfaces [4–6], basic issues such as the balance of forces acting on the interface and the influence of the incompressibility of the liquid enclosed by spherical interfaces have not yet been fully resolved. Curved interfaces of finite droplets pose the additional difficulty [7,8] that in the presence of external forces the condition of mechanical equilibrium demands to either fix the center of mass of the droplet by an external body force or to pin the droplet surface, for example, to a solid plate. The experimentally relevant issues of the boundary conditions at the plate and of their influence on the pair potential between capillary *monopoles* representing particles subjected to radial external forces have been studied previously [9,10]. Here we study the cases of capillary *dipoles* corresponding to particles subjected to external torques and of *higher* capillary multipoles corresponding to free particles with undulating three-phase contact lines (due to, e.g., nonspherical shapes of the particles or inhomogeneities of their surfaces). We derive the effective pair potentials for corresponding pointlike particles expressed as an expansion in terms of spherical harmonics. Within our model the particles are characterized by constant multipole moments, that is, independent of their spatial separation. Concerning flat interfaces the available experimental and numerical results reported in the literature indicate that in many cases this is a valid approximation [11,12]. If capillary monopoles are fixed by a constant external force acting on the particles in the direction perpendicular to the interface, such as gravity (or buoyancy [13]) or an electrostatic force [14], the free energy is dominated by the monopole-monopole term $\sim\ln(qd)$, where q^{-1} denotes the capillary length and d the spatial separation of the particles. If in addition the particles of size a are spherical and there are no external torques, the corrections to the leading monopole-monopole term in the effective capillary interaction potential are of the order $O(a/d)^4$ and thus negligible at separations $d/a \gg 1$ [15]. The assumption of constant monopoles cannot be applied in the case of particles protruding from a thin liquid film (such as a soap film [16] or a layer of liquid on a substrate [17]) of a thickness smaller than the particle diameters. In such a case the monopoles are modified due to the deformation of the interface induced by the other particle and thus detectably depend on the particle separation [16]. Force- and torque-free particles of nonspherical shape are sources of a deformation field characterized by the symmetry of the configuration of the three phase contact line. Generically, the first nonvanishing multipole is the quadrupole, which means that the interaction between free particles of irregular shape is dominated by the quadrupole-quadrupole term. The strength of this quadrupolar interaction increases with the amplitude of the undulation of the interface around the particle, which is usually more pronounced for elongated particles such as prolate ellipsoids or cylinders [at least for contact angles at their surface different from $\pi/2$ (see Ref. [18])]. However, in those cases higher capillary multipoles become important already at separations d of the order of several particle sizes [18,19]. These higher-order effects actually determine the equilibrium orientations of the particles close to contact [20–22] and their aggregation at high concentrations [23]. Actually, in the case of ellipsoids the expansion in terms of elliptic coordinates seems to be more appropriate than the usual multipole expansion [18].

Here our main goal is to study the effects of curvature on the interaction potentials between multipoles of arbitrary order. For monopoles and dipoles we find important qualitative differences from the case of a flat interface, in particular the occurrence of new local minima and metastable branches of the free energy, whereas in the case of quadrupoles we observe only minor quantitative differences. We note that an actual particle can always be associated with a set of multipoles, but

the issue of how this has to be implemented is beyond the scope of the present study. (Concerning a flat interface we refer to Refs. [6,21,23,24]). However, our full numerical calculations for actual particles reveal that in the cases with external forces and torques the point-multipole model performs very well. For ellipsoids apparently higher-order corrections are needed.

The paper is organized as follows. In Sec. II we study small deformations of a droplet in the presence of an external pressure field and in Sec. III we introduce Green's function for the linearized capillary equation on a sphere. In Sec. IV we derive a general formula for the interaction potentials and we focus on the cases of monopoles, dipoles, and quadrupoles. In Sec. V we compare these analytical results with those of the numerical free energy minimization (obtained by using the software SURFACE EVOLVER [25]). We discuss the results in Sec. VI.

II. PERTURBATION THEORY

We consider a spherical droplet of radius R_0 with colloidal particles trapped at its surface with surface tension γ. We model the effect of particles in terms of an external surface pressure field $\Pi(\Omega)$ (see below) parameterized by spherical coordinates $\Omega = (\theta,\phi)$ on the unit sphere. The equilibrium shape of the droplet subjected to the pressure field Π follows from minimizing the corresponding free energy functional $\mathcal{F}[\{v(\Omega)\}]$ expressed in terms of the dimensionless radial displacement of the interface $v(\Omega) = [r(\Omega) - R_0]/R_0$. In the limit of small interfacial gradients $|\nabla_a v| \ll 1$ one has [7,9]

$$\frac{1}{\gamma R_0^2}\mathcal{F}[\{v(\Omega)\}] = \int d\Omega \left[\frac{1}{2}(\nabla_a v)^2 - v^2 - (\pi(\Omega)+\mu)v\right], \tag{1}$$

where $\nabla_a := \boldsymbol{e}_\theta \partial_\theta + \frac{\boldsymbol{e}_\phi}{\sin\theta}\partial_\phi$ is the dimensionless angular gradient on the unit sphere [26]. The first two terms in Eq. (1) represent the surface free energy, the third term corresponds to the work done by the dimensionless external pressure $\pi(\Omega) = \Pi(\Omega)R_0/\gamma$ in displacing the interface, and the fourth term serves to implement the volume conservation. The value of the Lagrange multiplier $-\mu$ follows from imposing the volume constraint

$$\int d\Omega\, v = 0; \tag{2}$$

$\gamma\mu/R_0$ can be identified with the shift in the internal pressure of the droplet with respect to the Laplace pressure $2\gamma/R_0$ of an unperturbed, perfectly spherical droplet. The condition of mechanical equilibrium imposes an additional constraint on the pressure field,

$$\int d\Omega\, \pi(\Omega)\boldsymbol{e}_r = 0, \tag{3}$$

which expresses the balance of forces acting on the droplet. The stationary condition $\delta\mathcal{F}/\delta v = 0$ leads to the Euler-Lagrange equation

$$-\left(\nabla_a^2 + 2\right)v(\Omega) = \pi(\Omega) + \mu. \tag{4}$$

We expand both the deformation $v(\Omega)$ and the pressure field $\pi(\Omega)$ in spherical harmonics $Y_{lm}(\Omega)$ so that Eq. (4) turns into an infinite set of algebraic equations [27]:

$$[l(l+1) - 2]v_{lm} = \pi_{lm} + \mu\delta_{l0}, \tag{5}$$

where $l = 0,1,\ldots,$ and $m = -l,\ldots,l$, and the spherical multipoles are defined as $X_{lm} := \int d\Omega'\, X(\Omega')Y_{lm}(\Omega')$ for $X(\Omega) = v(\Omega)$ or $X(\Omega) = \pi(\Omega)$. The volume constraint in Eq. (2) implies $v_{00} = 0$ and thus $\mu = -\pi_{00}$, which means that the internal pressure shift counterbalances the external pressure. According to Eq. (5) the $l = 1$ components of the deformation v are undefined. This is consistent with the fact that those components describe translations of the whole droplet without any change in shape which do not change the free energy. On the other hand, all $l = 1$ components of the external pressure π must cancel, reflecting the condition of balance of forces acting on the droplet. Indeed, the multipoles $\pi_{1-1},\pi_{10},\pi_{11}$ are proportional to the Cartesian components f_x, f_y, f_z of the total force $\boldsymbol{f}$ acting on the droplet. Hence, the condition $\boldsymbol{f} = 0$ is equivalent to $\pi_{1m} = 0$ with $m = -1,0,1$.

III. GREEN'S FUNCTION AND BALANCE OF FORCES

In accordance with the above reasoning we consider a pressure field in the form of a superposition of N forces f_i acting pointlike into directions Ω_i and an additional contribution $\pi_{\text{c.m.}}(\Omega)$ which acts as to fix the center of mass (c.m.):

$$\pi(\Omega) = \sum_{i=1}^{N} q_i \delta(\Omega,\Omega_i) + \pi_{\text{c.m.}}(\Omega), \tag{6}$$

where $q_i := f_i/(\gamma R_0)$ and $\delta(\Omega,\Omega_i) = \delta(\theta-\theta_i)\delta(\phi-\phi_i)/\sin\theta_i$ is the Dirac δ distribution expressed in terms of spherical coordinates and where the pressure field $\pi_{\text{c.m.}}$ fulfills the condition $\sum_i^N \pi_{i,1m} + \pi_{\text{c.m.},1m} = 0$ for $m = -1,0,1$. The interface deformation due to the point forces can be written as a superposition of single particle contributions:

$$v(\Omega) = \sum_{i}^{N} q_i G(\Omega,\Omega_i), \tag{7}$$

where $G(\Omega,\Omega')$ is Green's function describing the response of the interface in direction Ω to a point force applied in direction Ω' and which, according to the constraints of constant liquid volume and fixed center of mass, fulfills the equation [27]

$$-\left(\nabla_a^2 + 2\right)G(\Omega,\Omega') = \sum_{l\geqslant 2}\sum_{m=-l}^{l} Y_{lm}^*(\Omega)Y_{lm}(\Omega'), \tag{8}$$

where the right-hand side is a modified Dirac δ function $\hat{\delta}(\Omega-\Omega')$ with the $l = 0$ and $l = 1$ components projected out. The vanishing of the $l = 0$ component of G reflects the condition of constant volume $\int d\Omega\, G(\Omega,\Omega') = 0$ [Eq. (2)], whereas the vanishing of the $l = 1$ component of G is due to the condition that the center of mass of the droplet is fixed in space, that is, $\int d\Omega\, \boldsymbol{e}_r G(\Omega,\Omega') = 0$ [see Eq. (3)], and due to the fact that $\boldsymbol{e}_r$ can be expressed in terms of spherical harmonics with $l = 1$ only.

We note that if $\pi_{\text{c.m.}}$ is due to a spatially constant body force it does not contribute to the deformation at all. Indeed, in this case all spherical harmonics components of $\pi_{\text{c.m.}}$ are zero other than those with $l = 1$ [28] so that the corresponding deformation $\int d\Omega' \pi_{\text{c.m.}}(\Omega') G(\Omega,\Omega')$ vanishes because upon construction $G(\Omega,\Omega')$ does not contain the $l = 1$ components. In the following we shall assume that $\pi_{\text{c.m.}}$ is due to a body force.

The expression in Eq. (7) for the deformation under the action of point forces can be generalized to the case of an arbitrary continuous force distribution $\tilde{\pi}(\Omega)$:

$$v(\Omega) = \int d\Omega' \, \tilde{\pi}(\Omega') G(\Omega,\Omega'). \tag{9}$$

We note that the total pressure π acting on the interface again encompasses the additional component $\pi_{\text{c.m.}}$ (such that $\pi = \tilde{\pi} + \pi_{\text{c.m.}}$ [30]), which, however, as discussed above, does not contribute to the deformation of the droplet.

One can express the free energy in terms of Green's function by integrating by parts Eq. (1), by using Eq. (4) and the divergence theorem, and finally by inserting $v(\Omega)$ as given by Eq. (9) [27]:

$$\frac{1}{\gamma R_0^2} F = -\frac{1}{2} \int d\Omega \int d\Omega' \, \tilde{\pi}(\Omega) G(\Omega,\Omega') \tilde{\pi}(\Omega'). \tag{10}$$

IV. CAPILLARY INTERACTIONS

A. Free energy in the presence of an external pressure distribution

We study the pressure $\tilde{\pi}$ localized around two different directions Ω_1 and Ω_2. To this end we introduce the following decomposition:

$$\tilde{\pi}(\Omega) = \pi_1\big(\hat{R}_1^{-1}\Omega\big) + \pi_2\big(\hat{R}_2^{-1}\Omega\big), \tag{11}$$

where $\hat{R}_1$ ($\hat{R}_2$) denotes the rotation transforming the original coordinate frame xyz into the coordinate frame $x'y'z'$ ($x''y''z''$), referred to as O_1 (O_2), associated with the pressure distribution π_1 (π_2) (see Fig. 1). We use the parametrization in terms of Euler angles, in which an arbitrary rotation $\hat{R}$ can be composed of a rotation around the z axis by the angle α, around the (rotated) y axis by the angle β, and finally around the (rotated) z axis by the angle γ. Under the rotation $\hat{R}(\alpha,\beta,\gamma)$ of the coordinate frame the coordinates transform according to $\hat{R}^{-1}$, as indicated in Eq. (11).

The total free energy can be written as $F = F_{1,\text{self}} + F_{2,\text{self}} + \Delta F$, where $F_{i,\text{self}} = -[f_i^2/(4\pi\gamma)] \ln(R_0/a_i) + O(1)$ is the self-energy of the pressure source π_i [9], which does not depend on the relative position of the sources on the droplet but depends on their spatial extent a_i. Taking the source to be located at the north pole, this is defined as the smallest distance for which $\pi_i(\theta,\phi) = 0$ for all $\theta > a_i/R_0$ and $\phi \in [0,2\pi)$; in the next section this corresponds to the solid angle circumscribing the particle-liquid interface. The interaction free energy ΔF is given by the cross terms in Eq. (10) with π from Eq. (11):

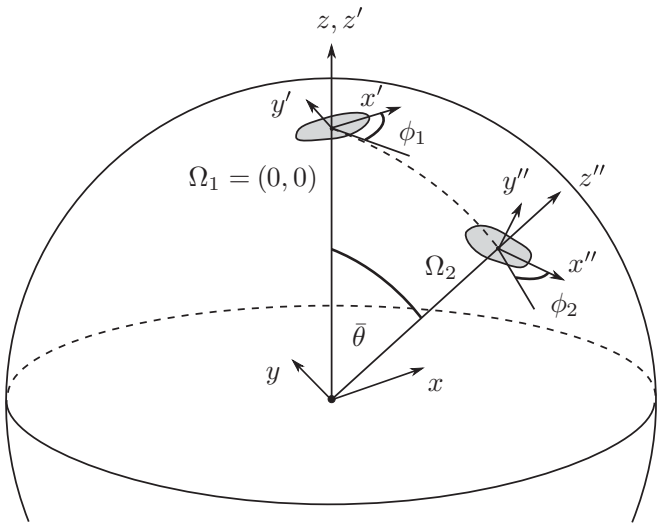

FIG. 1. Angular configuration of the pressure distributions symbolically represented as gray patches centered at the directions $\Omega_1 = (0,0)$ (north pole) and Ω_2 on the unit sphere. The angles ϕ_1 and ϕ_2 represent orientations of the local coordinate frames $x'y'z'$ and $x''y''z''$ associated with the pressure distributions (see main text).

$$\begin{aligned}\frac{1}{\gamma R_0^2}\Delta F &= -\int d\Omega \int d\Omega' \, \pi_1\big(\hat{R}_1^{-1}\Omega\big) G(\Omega,\Omega') \pi_2\big(\hat{R}_2^{-1}\Omega'\big) \\ &= -\int d\Omega \int d\Omega' \sum_{l,m} \pi_{1,lm} Y_{lm}^*\big(\hat{R}_1^{-1}\Omega\big) \\ &\quad \times \sum_{j,n} g_j Y_{jn}^*(\Omega) Y_{jn}(\Omega') \sum_{k,m'} \pi_{2,km'} Y_{km'}^*\big(\hat{R}_2^{-1}\Omega'\big),\end{aligned} \tag{12}$$

where

$$g_l = \begin{cases} 0 & \text{for} \quad l = 0,1, \\ \dfrac{1}{l(l+1)-2} & \text{for} \quad l \geqslant 2, \end{cases} \tag{13}$$

are the spherical harmonics coefficients of $G(\Omega,\Omega')$. Without loss of generality we can take $\Omega_1 = 0$ such that the reference frame O_1 coincides with the original reference frame xyz (see Fig. 1), which implies that $\hat{R}_1 = \mathbb{1}$.

Spherical harmonics transform under the representation of the group of rotations according to $Y_{lm}(\hat{R}^{-1}\Omega) = \sum_{m'=-l}^{l} D^l_{m',m}(\hat{R}) Y_{lm'}(\Omega)$, where $D^l_{m',m}$ is the Wigner D matrix and reads (adopting the convention used in Ref. [29])

$$D^l_{m',m}(\hat{R}) = D^l_{m',m}(\alpha,\beta,\gamma) = e^{-im'\alpha} d^l_{m',m}(\beta) e^{-im\gamma}, \tag{14}$$

where $d^l_{m',m}(\beta)$ is known as the Wigner (small) d matrix. We use the parametrization in terms of the orientations ϕ_1 and ϕ_2 of the coordinate frames O_1 and O_2, respectively, relative to the great circle connecting the points $\Omega_1 = 0$ and Ω_2 on the unit sphere (see Fig. 1). The rotation $\hat{R}_2$ is then parameterized by the triad of the Euler angles $(2\pi - \phi_1, \bar{\theta}, \phi_2)$. By using the orthogonality $\int d\Omega Y_{lm}(\Omega) Y^*_{l'm'}(\Omega) = \delta_{ll'}\delta_{mm'}$ of the spherical harmonics, and due to the identities $Y^*_{lm}(\Omega) = (-1)^m Y_{l,-m}(\Omega)$

and $D^{l}_{m',m}{}^{*}(\alpha,\beta,\gamma) = (-1)^{m-m'} D^{l}_{-m',-m}(\alpha,\beta,\gamma)$, we finally obtain

$$\frac{1}{\gamma R_0^2}\Delta F = -\sum_{l\geqslant 2}\sum_{m=-l}^{l}\sum_{m'=-l}^{l} \pi_{1,lm}\,\pi_{2,lm'}\,(-1)^{m'} \times g_l d^{l}_{m,-m'}(\bar{\theta})\, e^{i(m\phi_1+m'\phi_2)}. \tag{15}$$

B. Relation to colloidal particles in the limit of pointlike pressure distributions

Having in mind colloidal particles as sources of the effective surface pressure π, we would like to relate the spherical multipoles π_{lm}, $l \geqslant 0$, $m = -l,\ldots,l$, to capillary multipoles defined for the case of a flat interface which have a clear physical meaning. For example, the capillary monopole and dipole are given by the total external force and torque, respectively, acting on the particle and the capillary quadrupole is proportional to the amplitude of the three-phase contact line undulation at the particle surface [6]. For particle sizes $a \ll R_0$ the interface can be treated as being locally flat in the close neighborhood $\Delta\Omega$ of angular extent $O(a/R_0)$ around each individual particle. Assuming for reasons of simplicity that $\Delta\Omega$ is centered at the z axis and approximating it by a circular disk $D(a)$ of radius a in the tangent plane we can use the asymptotic form of spherical harmonics [31],

$$Y_{lm}(\theta,\phi) \xrightarrow[\theta\to 0]{} i^{|m|+m} A_{l|m|}\theta^{|m|} e^{im\phi}, \tag{16}$$

where

$$A_{ln} = \sqrt{\frac{2l+1}{4\pi}\frac{(l+n)!}{(l-n)!}}\frac{1}{2^n n!}, \quad n = 0,1,\ldots, \tag{17}$$

in order to obtain

$$\pi_{lm} = \int_{\Delta\Omega} d\Omega'\,\pi(\Omega')Y_{lm}(\Omega') \xrightarrow[a/R_0\to 0]{} \begin{cases} \sqrt{\dfrac{2l+1}{4\pi}}\left(\dfrac{a}{R_0}\right)Q_0, & m = 0, \\ i^{|m|+m}A_{l|m|}\left(\dfrac{a}{R_0}\right)^{|m|+1} Q_{|m|}e^{im\tilde{\phi}_{|m|}}, & m \neq 0, \end{cases} \tag{18}$$

where we have introduced the dimensionless moduli

$$Q_0 := \int_{D(a)} \frac{d^2x'}{a^2}\,\frac{a\Pi(z')}{\gamma}, \tag{19}$$

$$Q_n := \left|\int_{D(a)} \frac{d^2x'}{a^2}\,\frac{a\Pi(z')}{\gamma}\left(\frac{z'}{a}\right)^n\right|, \tag{20}$$

and the phase

$$\tilde{\phi}_n := \frac{1}{n}\arg\int_{D(a)} \frac{d^2x'}{a^2}\,\frac{a\Pi(z')}{\gamma}\left(\frac{z'}{a}\right)^n, \tag{21}$$

where $n = 1,2,\ldots$; z' denotes a complex number, and $\Pi(\boldsymbol{x}') \equiv \gamma\pi[\Omega'(\boldsymbol{x}')]/R_0$, with $\boldsymbol{x}'(\Omega')$ being a projection onto the plane tangent to the reference sphere at Ω_i. Equations (19) and (20) comprise the definitions of the capillary multipoles Q_n at a locally flat interface (see Refs. [6,11]). Accordingly, due to the conditions of force and torque balance on a flat interface [6], Q_0 represents a "capillary monopole," that is, the total external force acting on the particle, and Q_1 represents a "capillary dipole," that is, the total external torque. In the case of a free particle, Q_2 represents the lowest nonvanishing multipole. Furthermore, we note that for each particle i one can always choose the orientation ϕ_i of the coordinate frame O_i such that the phase of the order n vanishes, that is, $\tilde{\phi}_{i,n} = 0$. We can write the interaction energy $\Delta F_{nn'}$ for a pair of capillary multipoles Q_n and $Q'_{n'}$ of arbitrary orders $n \geqslant 0$ and $n' \geqslant 0$ as a sum of terms such that in Eq. (16) the sum over l is taken under the constraint $l \geqslant \max\{2,n,n'\}$ with m and m' fixed to $m = \pm n$ and $m' = \pm n'$; this implies $\Delta F = \sum_{n,n'=0}^{\infty}\Delta F_{nn'}$. Accordingly, the interaction free energy $\Delta F_{nn'}$ for a pair of capillary multipoles Q_n and $Q'_{n'}$ scales with the droplet radius R_0 as $\Delta F_{nn'} \sim \gamma a^{n+1}a'^{n'+1}/R_0^{n+n'}$. Note that in the case of two monopoles ($n = 0$ and $n' = 0$) the interaction does not depend on R_0 but only on the moduli Q_0 and Q'_0.

The Wigner d matrix in Eq. (15) can be expressed in terms of the Jacobi polynomials $P_n^{(\sigma,\rho)}(\cos\bar{\theta})$ [31]:

$$d^{l}_{m,m'}(\bar{\theta}) = \left[\frac{(l+m')!(l-m')!}{(l+m)!(l-m)!}\right]^{1/2}\left(\sin\frac{\bar{\theta}}{2}\right)^{m'-m} \times \left(\cos\frac{\bar{\theta}}{2}\right)^{m'+m} P_{l-m'}^{(m'-m,m'+m)}(\cos\bar{\theta}). \tag{22}$$

By using certain properties of the Jacobi polynomials (see, e.g., Ref. [31]), we finally obtain

$$\frac{\Delta F_{nn'}}{\gamma a a'} \xrightarrow[a/R_0,a'/R_0\to 0]{} \frac{Q_n Q'_{n'}}{(-2)^{n+n'+1}n!n'!\pi}\frac{a^n a'^{n'}}{R_0^{n+n'}}\sum_{l\geqslant\max\{2,n,n'\}}\frac{(2l+1)}{(l+2)(l-1)}$$

$$\times \begin{cases} \dfrac{(l+n')!}{(l-n)!}\Big[(-1)^n\cos(n\phi_1+n'\phi_2)\left(\cos\dfrac{\bar{\theta}}{2}\right)^{n'-n}\left(\sin\dfrac{\bar{\theta}}{2}\right)^{n'+n} P_{l-n'}^{(n'+n,n'-n)}(\cos\bar{\theta}) \\ \quad +\cos(n\phi_1-n'\phi_2)\left(\cos\dfrac{\bar{\theta}}{2}\right)^{n'+n}\left(\sin\dfrac{\bar{\theta}}{2}\right)^{n'-n} P_{l-n'}^{(n'-n,n'+n)}(\cos\bar{\theta})\Big], & n>0,\quad n'>0, \\ (-1)^n\cos(n\phi_1)P_l^n(\cos\bar{\theta}), & n>0,\quad n'=0, \\ 2^{-1}P_l(\cos\bar{\theta}), & n=0,\quad n'=0, \end{cases} \tag{23}$$

where P_l and P_l^n are the Legendre and the associated Legendre polynomials, respectively.

C. Effective interaction potentials

For simplicity, we evaluate the interaction energy in Eq. (23) for $a = a'$ and $n' = n$. In the case of two identical pointlike *monopoles*, $n = n' = 0$, one obtains [32]

$$\frac{\Delta F_{00}(\bar{\theta})}{\gamma a^2} \xrightarrow[a/R_0 \to 0]{} \frac{Q_0^2}{4\pi}\left[\frac{1}{2} + \frac{4}{3}\cos\bar{\theta} + 2\cos\bar{\theta}\ln\left(\sin\frac{\bar{\theta}}{2}\right)\right], \tag{24}$$

which gives Green's function $G(\bar{\theta}) \equiv -\Delta F_{00}(\bar{\theta})/(\gamma a^2 Q_0^2)$ as first derived in Ref. [27]. We note that according to Eq. (24) one has $G(\bar{\theta} \to 0) \to -[1/(2\pi)]\ln\bar{\theta}$ [see the dashed line in Fig. 2(a)], which renders the deformation $v(r) = -[1/(2\pi)]\ln(r/R_0)$ due to a pointlike force, known for a flat interface, where $r = \bar{\theta}R_0 \ll R_0$ is the arc length (see the dashed line in Fig. 1) and R_0 plays the role of the capillary length.

In the case of pointlike *dipoles*, $n = n' = 1$, one can evaluate the series involving the Jacobi polynomials by using their generating function (see Appendix A):

$$\frac{1}{\gamma a^2}\Delta F_{11}(\bar{\theta},\phi_1,\phi_2) \xrightarrow[a/R_0 \to 0]{} \frac{Q_1^2}{8\pi}\left(\frac{a}{R_0}\right)^2 [\cos(\phi_1+\phi_2) f_+(\bar{\theta}) + \cos(\phi_1-\phi_2) f_-(\bar{\theta})], \tag{25}$$

where ϕ_1 and ϕ_2 are the orientations of the particles as indicated in Fig. 1 and chosen such that the phases $\tilde{\phi}_{i,n}$ defined in Eq. (21) vanish for $n = 1$ and where

$$f_+(\theta) := \frac{1}{\sin^2(\theta/2)} - 4\sin^2\frac{\theta}{2}\ln\left(\sin\frac{\theta}{2}\right) - \frac{20}{3}\sin^2\frac{\theta}{2} + 2, \tag{26}$$

$$f_-(\theta) := 4\left(\cos\frac{\theta}{2}\right)^2\ln\left(\sin\frac{\theta}{2}\right) + \frac{20}{3}\cos^2\frac{\theta}{2}. \tag{27}$$

We note that the dependences on the angular separation $\bar{\theta}$ and on the orientations ϕ_1, ϕ_2 do not factorize. Therefore, in order to minimize the free energy, the particles adopt orientations which depend on $\bar{\theta}$. According to Eq. (28) below, one can distinguish three branches of the free energy [see the dotted lines in Fig. 3(a)] corresponding to three different minimal orientations, out of which the one with the lowest free energy is the equilibrium one. Assuming that the rotational relaxation of the particles is much faster than the translational one, an effective interaction potential can be obtained by minimizing the free energy with respect to ϕ_1 and ϕ_2:

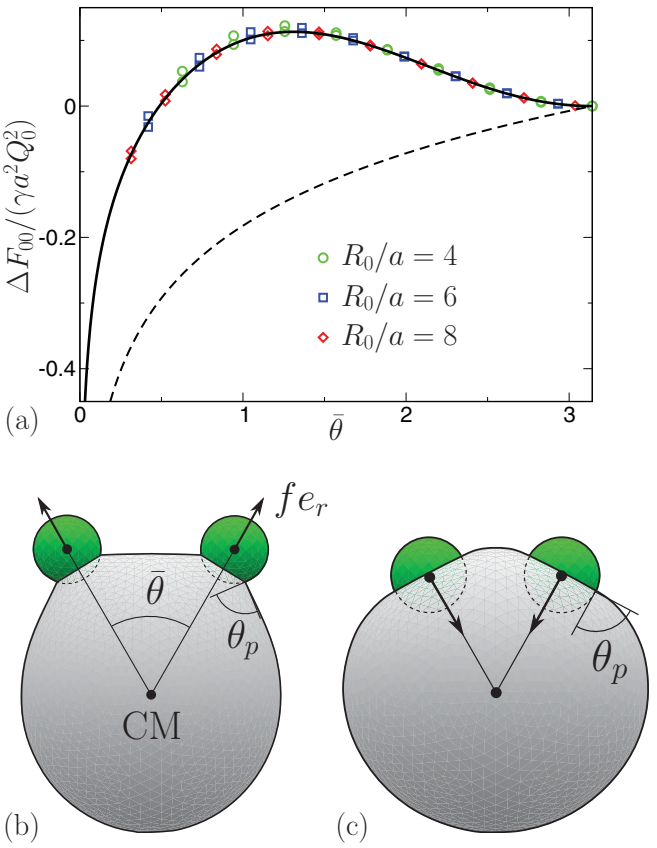

FIG. 2. (Color online) (a) Rescaled effective interaction potential [Eq. (24), solid line] between two capillary monopoles. The level of zero energy is shifted such that $\Delta F_{00}(\bar{\theta} = \pi) = 0$. The dashed line corresponds to the expression $[\ln(\bar{\theta}) - \ln(\pi)]/(2\pi)$ representing for comparison the case of a flat interface with the equivalent spatial separation $d = R_0\bar{\theta}$ of the particles. As expected, for $\bar{\theta} \to 0$ the full curve approaches the dashed curve. The symbols correspond to the results of the numerical minimization of the free energy for droplets of various radii, with the contact angle at the particle $\theta_p = \pi/2$, and with the strength of the external force $Q_0 = f/(\gamma a) = -1$ (upper set of symbols at a given $\bar{\theta}$) or $Q_0 = f/(\gamma a) = 1$ (lower set of symbols), respectively. The data terminate at an angular separation corresponding to the contact of the particles. In (b) and (c) we show snapshots of the triangulated droplet surface corresponding to $R_0/a = 4$, $\theta_p = \pi/2$, and $Q_0 = 2$ (b) or $Q_0 = -2$ (c) with the position of the center of mass of the liquid indicated by CM. In (b) and (c) a cross-sectional view is shown with the plane defined by CM and the centers of the particles.

$$\frac{1}{\gamma a^2}\min_{\{\phi_1,\phi_2\}}\{\Delta F_{11}(\bar{\theta},\phi_1,\phi_2)\} \xrightarrow[a/R_0 \to 0]{} \frac{Q_1^2}{8\pi}\begin{cases} -f_+(\bar{\theta}) + f_-(\bar{\theta}) & \text{for} \quad \bar{\theta} < \bar{\theta}_0, & \uparrow\uparrow \quad \text{or} \quad \downarrow\downarrow, \\ -f_+(\bar{\theta}) - f_-(\bar{\theta}) & \text{for} \quad \bar{\theta}_0 < \bar{\theta} < \bar{\theta}_1, & \leftarrow\rightarrow \quad \text{or} \quad \rightarrow\leftarrow, \\ f_+(\bar{\theta}) - f_-(\bar{\theta}) & \text{for} \quad \bar{\theta} > \bar{\theta}_1, & \uparrow\downarrow \quad \text{or} \quad \downarrow\uparrow, \end{cases} \tag{28}$$

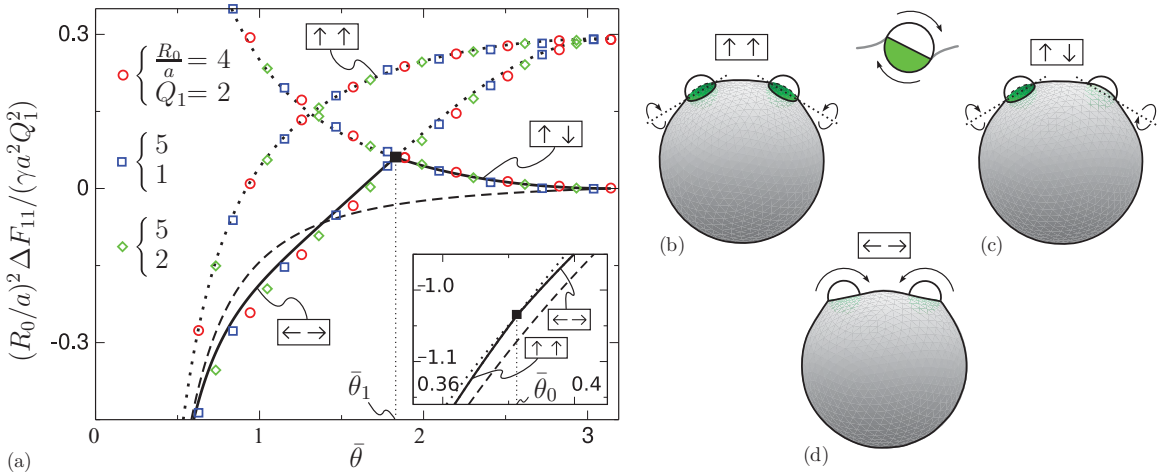

FIG. 3. (Color online) (a) Rescaled effective interaction potential [Eqs. (25)–(28), solid lines] between two capillary dipoles. The dashed line corresponds to the expression $(1/\pi^2 - 1/\bar{\theta}^2)/(2\pi)$ representing for comparison the case of a flat interface with the equivalent spatial separation $d = R_0\bar{\theta}$ of the particles. The dotted lines represent three metastable branches of the free energy [see Eq. (28)] corresponding to three different orientations of the particles with two relevant intersection points [at $\bar{\theta}_1 \simeq 1.83$, where $f_+(\bar{\theta}_1) = 0$, and $\bar{\theta}_0 \simeq 0.38$, where $f_-(\bar{\theta}_0) = 0$] indicated by solid squares. In each interval $[0,\bar{\theta}_0]$, $[\bar{\theta}_0,\bar{\theta}_1]$, and $[\bar{\theta}_1,\pi]$ the full curve corresponds to the lowest of the branches and as such describes thermal equilibrium. The symbols correspond to the numerical results with a finite-size correction (see main text) applied in the case $\leftarrow\rightarrow$. In (b)–(d) we show the snapshots of the numerically calculated droplet shapes corresponding to $R_0/a = 5$ and $\bar{\theta} = \pi/3$; the unstable configuration (b) corresponds to the local maximum of the free energy with respect to the orientations of the particles, the metastable configuration (c) to the inflection point, and the stable one (d) to the local minimum. The stability of the branches changes discontinuously at the intersection points. In (b) and (c) the green parts denote the fixed area of the particle-liquid interface with a fixed three phase contact line.

where $\bar{\theta}_0 = \arccos[1 - 2\exp(-10/3)] \simeq 0.38$ and $\bar{\theta}_1 \simeq 1.83$ are the zeros of $f_-(\bar{\theta}_0) = 0$ and $f_+(\bar{\theta}_1) = 0$, respectively; the arrows indicate the minimal orientational configuration. (The tips of the arrows indicate the direction in which the effective pressure is positive, or, equivalently, the direction of the positive tilt of the particle, so that, for example, ↑ ↑ corresponds to $\phi_1 = \pi/2$ and $\phi_2 = \pi/2$, etc.)

In the case of pointlike *quadrupoles*, $n = n' = 2$, one obtains (see Appendix A)

$$\frac{1}{\gamma a^2}\Delta F_{22}(\bar{\theta},\phi_1,\phi_2) \xrightarrow[a/R_0\to 0]{} -\frac{3Q_2^2}{64\pi}\left(\frac{a}{R_0}\right)^4 \cos(2\phi_1+2\phi_2) \times \frac{1}{\sin^4(\bar{\theta}/2)}. \tag{29}$$

Distinct from the case of dipoles, the free energy has a minimum for $\phi_1 + \phi_2 = k\pi, k = 0,1,\ldots$ [which implies $\cos(2\phi_1 + 2\phi_2) = 1$] independently of $\bar{\theta}$, so that

$$\frac{1}{\gamma a^2}\min_{\{\phi_1,\phi_2\}}\{\Delta F_{22}(\bar{\theta},\phi_1,\phi_2)\} \xrightarrow[a/R_0\to 0]{} -\frac{3Q_2^2}{64\pi}\left(\frac{a}{R_0}\right)^4 \times \frac{1}{\sin^4(\bar{\theta}/2)}. \tag{30}$$

This corresponds to a monotonic attraction [see the thick solid line in Fig. 4]. We note that the corresponding asymptotic form $\Delta F_{22} = -[3Q_2^2/(4\pi)][a/(R_0\bar{\theta})]^4$ of the interaction potential, which is strictly valid only in the limit $\bar{\theta} \ll 1$, is actually a good approximation at all angular separations [see the black dashed line in Fig. 4(a)].

V. NUMERICAL RESULTS

In this section we compare our approximate analytic theory with the numerical minimization of the free energy for colloidal particles floating at the surface of a droplet. We employ a method based on steepest descent [25] in order to study spherical particles subjected to external forces and torques as well as the case of free ellipsoidal particles. The numerical procedure consists of the iterative evolution of a body of liquid from a predefined initial configuration, which is as simple as possible (e.g., a cube), under given constraints at the particle surfaces and preserving the volume of liquid. The triangulated liquid surface evolves toward the equilibrium shape following the steepest descent of the free energy given by the following functional:

$$\mathcal{F}[\{\boldsymbol{r}(\Omega)\},h_1,h_2,\psi_1,\psi_2;\bar{\theta},\phi_1,\phi_2,f_1,f_2,T_1,T_2,\theta_p,a,V_l,\lambda] = \gamma S_{lg} + \sum_{i=1,2}(-\gamma\cos\theta_p S_{pl,i} - f_i h_i - \boldsymbol{T}_i\cdot\boldsymbol{\psi}_i) - \lambda(V - V_l). \tag{31}$$

The above functional is minimized with respect to the shape of the interface $\{\boldsymbol{r}(\Omega)\}$, the immersions of the particles h_i, and their tilts $\psi_i = |\boldsymbol{\psi}_i|$ while the angular separation $\bar{\theta}$ and the tangential orientations ϕ_i are kept fixed. The immersions can be defined with respect to an arbitrary reference radial position, the choice of which is of no importance because the free energy depends only on their relative changes. For simplicity we adopt the spherical drop without the particles and with radius R_0 as the reference configuration. Each tilt vector $\boldsymbol{\psi}_i$ is determined by the direction of the axis of tilt and the tilt angle ψ_i. The axis lies in the plane perpendicular to

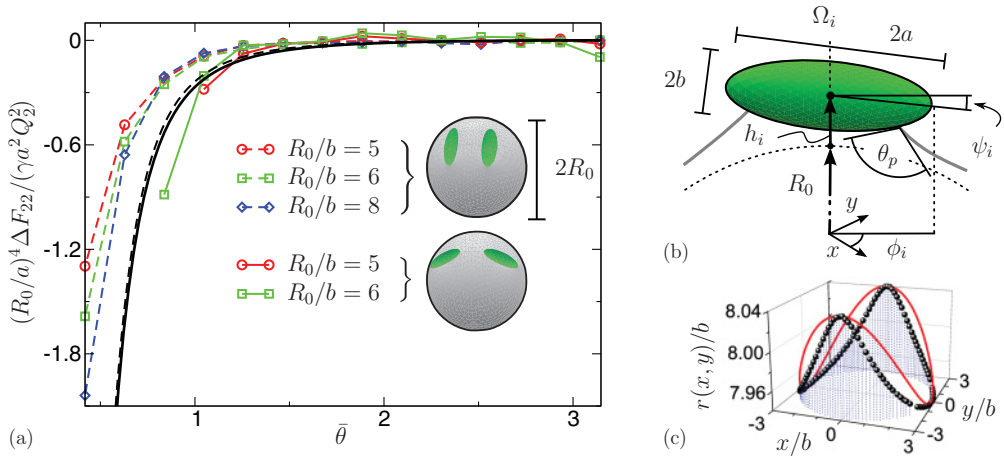

FIG. 4. (Color online) (a) Rescaled effective interaction potential between two capillary quadrupoles [Eq. (30), thick solid line]. The black dashed line corresponds to the expression $3(1/\pi^4 - 1/\bar{\theta}^4)/(4\pi)$ representing for comparison the case of a flat interface with the equivalent spatial separation $d = R_0\bar{\theta}$ of the particles. The symbols correspond to the results of the numerical minimization of the free energy for two force- and torque-free ellipsoidal particles with aspect ratio $a/b = 3$, contact angle $\theta_p = 2\pi/3$, various droplet radii R_0, and two different orientational configurations: tip-to-tip (full lines) and side-to-side (dashed lines), as visualized by the snapshots shown as insets. In view of large relative numerical errors for small values of ΔF_{22} the zero of the free energy is taken as a mean value of the data points with $\bar{\theta} > 1.5$. The colored lines connecting the symbols are guides to the eye. The variables describing the spatial configuration of particle i are explained in (b). The immersion h_i and the tilt angle ψ_i of the long axis of the particle with respect to the plane perpendicular to the direction Ω_i are both subjected to minimization, while the orientation ϕ_i is kept fixed. (c) Contour of the interface around a single particle at the north pole of a droplet, with $R_0/b = 8$ and for $\phi_i = \pi/2$, quantified in terms of the radial position $r(x,y)$ of the interface (symbols) at a fixed distance (equal to $3b$) from the particle center. For comparison the corresponding undulation $(\Delta u/2)\cos(2\phi)$, with the amplitude $\Delta u/b = 0.102$ chosen to be the same and with $\phi = \arctan(y/x)$, for a pure quadrupole placed at the particle center is plotted as the full red line.

the direction Ω_i and is determined by the orientation ϕ_i of the particle i [see, cf., Fig. 4(b)]. Accordingly, the rotations around Ω_i are frozen in so that one has to perform independent calculations for various ϕ_i in order to be able to compare their free energies. S_{lg} is the area of the liquid-gas interface and $S_{pl,i}$ are the areas of the particle-liquid interfaces. For convenience we assume that the contact angle θ_p on both particles is the same. The shape of the particles enters as an implicit parameter, and we assume that both particles are of identical shape and size (the latter denoted by a). The third and the fourth term in Eq. (31) represent minus the work done by the external forces f_i and torques $\boldsymbol{T}_i$, respectively, in shifting and rotating the particles, whereas the last term ensures conservation of the liquid volume V_l with λ as the corresponding Lagrange multiplier. In the cases with nonvanishing torques we consider pinned contact lines at the particle surfaces, which implies $S_{pl,i} = \text{const}$ so that the value of θ_p is actually irrelevant in those cases (for further explanations, see below). In all cases studied the center of mass of the droplet is fixed at the origin of the coordinate system, that is, at the center of the droplet without particles (which forms a perfect sphere).

In Fig. 2 we compare the numerical results for two spherical particles subjected to radial external forces ($f_1 = f_2 = f$) in the absence of torques ($T_i = 0$) with the analytical results for pointlike monopoles of strength $Q_0 = f/(\gamma a)$. Due to the mirror symmetry of the system, it is sufficient to determine only one half of the droplet with one of two particles. (The corresponding case of a hemispherical droplet sitting on a planar substrate with contact angle $\theta_0 = \pi/2$ has been thoroughly studied in Ref. [9].) In the present case of a full droplet the free energy is simply twice the free energy of a sessile droplet. We note that for the droplet sizes $R_0/a = \{4,6,8\}$ the agreement with the theoretical expression in Eq. (24) for pointlike dipoles is only achieved after subtracting from the numerical results a correction $\delta F_{00}/(\gamma a^2) = -Q_0(a/R_0)^2\cos^2(\bar{\theta}/2)$ accounting for the work done by the external force in displacing the center of mass of the droplet when the configuration of the immersed parts of the particles changes [33]. With this finite-size correction taken into account the agreement is almost perfect, which indicates that the higher-order multipoles induced by the particles are negligible.

Similarly, from Fig. 3 it follows that the numerical results for particles subjected to external torques ($|\boldsymbol{T}_1| = |\boldsymbol{T}_2| = T$) in the absence of forces ($f_i = 0$) are almost perfectly reproduced by the analytic model with capillary pointlike dipoles of strength $Q_1 = T/(\gamma a^2)$ [34]. We study spherical particles with the three phase contact lines pinned at the particle equators which prevents sliding of those lines on the particle surfaces. Physically, such a pinning can be accomplished by using so-called Janus particles composed of two hemispheres of different wettability. In the case of the configuration $\leftarrow\rightarrow$ ($\phi_1 = \pi, \phi_2 = 0$) a semiempirical finite-size correction $\delta F_{11}/(\gamma a^2) = Q_1(a/R_0)^3\sin\bar{\theta}$ is subtracted from the numerically calculated free energy in order to facilitate comparison with Eqs. (26)–(28). [This correction does not apply to the other two branches $\uparrow\ \uparrow$ and $\uparrow\ \downarrow$ (see Appendix B).] We have checked the validity of this correction for $Q_1 = 1,2$ and droplet radii $R_0/a = 4,5$, and 8 (the case $R_0/a = 8$ is not shown in Fig. 3). For $R_0/a \lesssim 5$ and at large angular separations the correction is comparable with

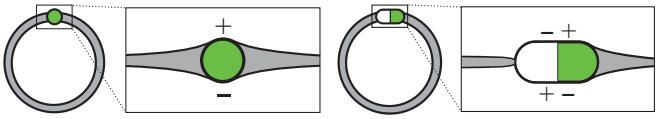

FIG. 5. (Color online) Particles inside thin spherical liquid films (double droplets or bubbles). (a) A trapped spherical hydrophilic particle corresponds to two capillary monopoles of positive (+) and negative (–) sign induced at the external and at the internal interface of the film, respectively. (b) An elongated particle with a hydrophilic and a hydrophobic part corresponds, accordingly, to two capillary dipoles with opposite orientations, one at each side of the film. In both cases the sum of all the monopoles or dipoles associated with the particle at both interfaces is zero due to the condition that there are no external forces or torques acting on the particle.

the gap between the metastable branches of the free energy. Accordingly, in those cases the finite size of the particles may affect the stability of individual branches and the equilibrium orientations of the particles. However, the effect becomes negligible for larger droplets [35].

Finally, we consider freely floating prolate ellipsoidal particles with semiaxes a and b, $a > b$ (Fig. 4). The maximal size of the droplets accessible in our numerical calculations is limited by the relative numerical errors, which for $R_0/b \gtrsim 8$ become so large that they actually smear out the angular dependence of the free energy. (The errors grow $\sim R_0^4$, that is, much faster than $\sim R_0^2$, as in the case of dipoles; in the case of monopoles the errors practically do not depend on R_0.) For the same reason we consider only particles with a large aspect ratio ($a/b = 3$) for which the undulation of the contact line $\Delta u/a$ [see Fig. 4(c)] is large enough so that the amplitude of the free energy dominates over the numerical noise. In order to facilitate comparison with the analytic theory [Eq. (30)], the capillary quadrupole of each particle is approximated by the expression $Q_2 = 2\pi\,\Delta u/a$, where $\Delta u \equiv \max_\phi r(\theta = a/R_0,\phi) - \min_\phi r(\theta = a/R_0,\phi)$ is the undulation of the interface at the angular distance $\theta = a/R_0$ from the center of a single particle placed at the north pole of the droplet [see Fig. 4(c)]. The above relation between Q_2 and Δu is approximately valid for a single particle at a flat interface [6]. As an approximation for a droplet we adopt the same relation, $Q_2(R_0) = 2\pi\,\Delta u(R_0)/a$, with the radius-dependent undulation $\Delta u(R_0)$. This undulation has been calculated numerically for droplets with three different radii: $\Delta u(R_0/b = 5)/a = 0.028$, $\Delta u(R_0/b = 6)/a = 0.031$, $\Delta u(R_0/b = 8)/a = 0.034$. Here R_0 is the radius of the droplet *without* the particles. According to the data shown in Fig. 4(a) the effective interactions between two identical ellipsoids are monotonically attractive for both their tip-to-tip and side-to-side orientation. In the latter case the particles can approach each other closer and therefore this configuration at contact corresponds to the global minimum of the free energy. However, at a fixed angular separation the free energy is actually lower for the tip-to-tip configuration. The overall scaling of the free energy $\sim(R_0/a)^{-4}$ is observed at intermediate angular separations. At small separations the scaling breaks down while at large separations the accuracy of the data is insufficient to confirm this scaling. A more detailed comparison of these results with the analytic theory for point quadrupoles is discussed in the following section.

VI. DISCUSSION AND CONCLUSIONS

First, we discuss the influence of the curvature of the interface on the interaction potentials by comparing the expressions for the curved interfaces [Eqs. (25)–(29) and solid lines in Figs. 2–4] with the well established results for a flat interface (see, e.g., Ref. [11], dashed lines in Figs. 2–4), where the corresponding spatial separation d between the particles is given by $d = R_0\bar{\theta}$. A striking difference is the nonmonotonicity for curved interfaces of the free energy for monopole-monopole and dipole-dipole interactions, which in both cases leads to short-ranged attraction and long-ranged repulsion. The monopoles are apparently attracted toward one of the two configurations in which the particles stretch the droplet along a single direction, that is, when the particles are either in close contact or when they are at opposite antipodes of the droplet. In each of those two configurations the radial displacement of the particles is locally largest, which corresponds to the maximal work fh done by the external force f on each particle. This, in turn, corresponds to the local minima of the free energy. In contrast, in the case of dipoles the branches of the free energy for given orientational configurations of the particles vary monotonically. It turns out that the locally minimal orientations [$\uparrow\ \uparrow$, i.e., $\phi_1 = \pi/2, \phi_2 = \pi/2$ for small angular separations and $\uparrow\ \downarrow$, i.e., $\phi_1 = \pi/2, \phi_2 = -\pi/2$ for large ones; see Eq. (28), Fig. 3(a) and inset therein] are those in which the external torques acting on the particles add up so that their effect on the droplet is maximized. As such, in general, the nonmonotonicity of the free energy can be traced back to the presence of external forces or torques. We note that for $n = 0, 1$ the expected reduction of the results for curved interfaces to those for a flat interface occurs only for very small angular separations. This is not the case for quadrupoles ($n = 2$), for which at all separations there is no qualitative discrepancy and only a minor quantitative difference from the flat limit. Interestingly, in the case of dipoles ($n = 1$), our results indicate that the equilibrium orientation of the particles is sensitive to the curvature of the interface even for $\bar{\theta} \ll 1$, that is, in the limit of very large droplets and a fixed interparticle separation. It turns out that an infinitesimal curvature lifts the degeneracy of the free energy (as compared to the flat case) with respect to the configurations $\uparrow\ \uparrow$ ($\phi_1 = \pi/2, \phi_2 = \pi/2$) and $\leftarrow\ \rightarrow$ ($\phi_1 = \pi, \phi_2 = 0$) pointing toward the former as the one corresponding to the global minimum [see the inset in Fig. 3(a)]. Accordingly, the orientation of the particles serves as a probe of the curvature. However, this is not the case for pure quadrupoles, for which the analogous degeneracy is not lifted. In our arrow notation the configurations $\leftrightarrow\leftrightarrow$, $\updownarrow\ \updownarrow$, and the remaining ones for which $\phi_1 + \phi_2 = \pi$ are all equivalent; that is, they have the same free energy independent of the curvature. This degeneracy is lifted for actual ellipsoidal particles but not due to the finite curvature but, as discussed below, due to the presence of higher-order multipoles.

Now we compare the analytic theory with the numerical results for particles of extended size. Very good agreement between both methods for particles subjected to forces and torques (Figs. 2 and 3) indicates that in these cases higher capillary multipoles are negligible. However, they become important in the case of freely floating ellipsoidal particles. The

effective potentials (Fig. 4) obtained numerically for prolate spheroids with aspect ratio $a/b = 3$ and droplet radii $R_0/b = 5,6,8$ differ for particles oriented tip to tip ($\phi_1 = \phi_2 = 0$) and side to side ($\phi_1 = \phi_2 = \pi/2$). This, as already mentioned, signals the importance of capillary multipoles higher than a quadrupole, because the point-quadrupole approximation yields the same free energy for both orientations [see Eq. (30)]. The deviation from the quadrupole approximation manifests itself also in the undulation of the interface around a single ellipsoid which deviates significantly from the one corresponding to a pure quadrupole [see Fig. 4(c)]. Accordingly, having in mind that for the studied droplet sizes the spatial separation between the particles never exceeds several multiples of the long axis of the particle, the observed discrepancies in the free energy relative to the point-quadrupole approximation are actually not surprising. The additional dependence on the orientations revealed by our numerical calculations, which goes beyond the quadrupole approximation, resembles that of the well established case of a flat interface, which has been analyzed experimentally [19] and theoretically [18] in terms of a multipole expansion. Those studies showed that the point-quadrupole approximation, within which tip-to-tip and side-to-side configurations have the same free energy, is reliable only either for particles with a very small eccentricity ($b \simeq a$) or at large spatial separations $d \gg a$. Otherwise, one should rather consider an expansion in terms of elliptic coordinates, from which it follows that at a fixed spatial separation the tip-to-tip configuration is energetically more favorable [18]. This prediction agrees with the experimental observations [19]. Our numerical calculations indicate that also in the case of spherically curved interfaces the same configuration is the preferred one. However, we have not analyzed all possible orientations. In this context it is noteworthy that optimal orientations other then tip to tip and side to side have been observed at a flat interface for a pair of ellipsoidal particles of *different* sizes [20].

Finally, we propose an experimental setup for realizing capillary monopoles and dipoles bound to a spherically curved interface. To this end we consider a particle which is confined inside a spherical film, like the one formed by a soap bubble. If the diameter of the particle exceeds the film thickness, the boundary condition of a given contact angle at the particle surface imposes deformations of both the internal and the external surface of the film around the particle [see Fig. 5(a)]. The resulting long-ranged deformations correspond to those due to one capillary monopole induced at each side of the film. They have the same amplitude but the opposite sign so that the normal forces on the particle in the film add up to zero; for a similar setup in the case of a flat film, see also Refs. [16] and [11]. However, without an additional restoring force in both setups the total force on each interface separately is not balanced. In the case of a flat film mechanical equilibrium is restored by pinning both interfaces, for example, at a rectangular frame. In the case of a spherical bubble another mechanism is required, such as viscous friction of the liquid inside the film. The viscosity generates so-called lubrication forces [36] which for thin films asymptotically grow as the inverse thickness of the film, thus preventing its thinning. In the case of a thin spherical film constituting the bubble this leads to an effective fixing of the center of mass of the bubble [37]. Equivalently, instead of an air-water-air system one can also study an oil-water-oil system, that is, a droplet in a droplet. Highly stable double droplets (or ensembles of thereof, frequently referred to as double emulsions) can be produced and manipulated in microfluidic devices. This has been already demonstrated by various authors (for recent assessments see, e.g., Ref. [38]). In particular, it is possible to control the thickness of the liquid shell and therefore, indirectly, also the strength of the monopoles. Introducing colloidal particles or droplets of high surface tension into the shell appears to be experimentally feasible.

Obtaining capillary dipoles calls for more sophisticated particle structures. For this purpose one can use elongated shapes, for example, prolate ellipsoids or capped cylinders, which minimize their surface free energy by aligning their long axis tangentially to the interfaces of the film. If in addition those particles have two halves of different wettability chosen such that the regions of positive and negative deformation of the adjacent liquid interfaces occur at the opposite poles of the particle, these particles would correspond to capillary dipoles [see Fig. 5(b)]. Again, we assume that the corresponding torques on each interface of the film are balanced by the viscous friction of the liquid inside the film. One has to choose the system parameters carefully in order to minimize the effect of the associated capillary monopoles which otherwise would dominate the free energy. (As already mentioned, the sum of monopoles associated with the particle at both interfaces is always zero due to the condition of balance of forces acting on the particle but the capillary interactions with another particle are actually calculated for each interface separately; therefore, one has to avoid residual monopoles induced at each interface separately.) To this end one should arrange for contact angles $\pi/2 - \delta\theta$ and $\pi/2 + \delta\theta$, with arbitrary but not too large $\delta\theta$, on the hydrophilic and the hydrophobic parts, respectively.

In both cases described above the proposed setup renders monopoles and dipoles which are not constant because they are not fixed by external forces or torques. Instead, they are induced at the particles according to the local film thickness which in turn is a function of the spatial separation between the interacting particles. This slightly modifies the power law for the distance dependence of the capillary interactions. (In the case of a flat film this modification, being of the order of a few percent, has been even measured experimentally [16].) Our theoretical framework can be extended to such a case of distance-dependent effective multipoles.

ACKNOWLEDGMENTS

J.G. acknowledges financial support from the Polish Ministry of Sciences under the grant Iuventus Plus nr IP2010/012270.

APPENDIX A: CALCULATION OF SERIES CONTAINING JACOBI POLYNOMIALS

In Eq. (23) for $n = n' = 1$ the following series appears:

$$S_1^{(\sigma_1,\rho_1)}(x) := \sum_{j\geqslant 1} \frac{(j+1)(j+2)(2j+3)}{j(j+3)} P_j^{(\sigma_1,\rho_1)}(x), \quad \text{(A1)}$$

where $(\sigma_1,\rho_1) = (2,0)$ or $(0,2)$, and for $n = n' = 2$:

$$S_2^{(\sigma_2,\rho_2)}(x) := \sum_{j\geqslant 0}(j+2)(j+3)(2j+5)P_j^{(\sigma_2,\rho_2)}(x), \quad \text{(A2)}$$

where $(\sigma_2,\rho_2) = (4,0)$ or $(0,4)$. Those series can be evaluated using the generating function [39]:

$$g^{(\sigma,\rho)}(x,z) = \frac{1}{R(1-z+R)^{\sigma}(1+z+R)^{\rho}} = \sum_{n=0}^{\infty}\frac{z^n P_n^{(\sigma,\rho)}(x)}{2^{\sigma+\rho}}, \quad \text{(A3)}$$

where $R = \sqrt{1-2xz+z^2}$ and $|z| < 1$. One finds the relationships

$$S_1^{(\sigma_1,\rho_1)}(x) = 2\int_0^1 dy\, y^2 \int_0^y dz\, z^{-2}\frac{\partial}{\partial z}z^{1/2}\frac{\partial}{\partial z}z^2\frac{\partial}{\partial z}z \times [2^{\sigma_1+\rho_1}g^{(\sigma_1,\rho_1)}(x,z)-1] \quad \text{(A4)}$$

and

$$S_2^{(\sigma_2,\rho_2)}(x) = 2^{\sigma_2+\rho_2+1}\lim_{z\to 1}\frac{\partial}{\partial z}z^{1/2}\frac{\partial}{\partial z}z^2\frac{\partial}{\partial z}z^2 g^{(\sigma_2,\rho_2)}(x,z), \quad \text{(A5)}$$

which can be evaluated with the results

$$S_1^{(2,0)}(x) = \frac{4}{(1-x)^2}+\frac{4}{1-x}-2\ln\left(\frac{1-x}{2}\right)-\frac{20}{3}, \quad \text{(A6)}$$

$$S_1^{(0,2)}(x) = -2\ln\left(\frac{1-x}{2}\right)-\frac{20}{3}, \quad \text{(A7)}$$

$$S_2^{(4,0)}(x) = \frac{96}{(1-x)^4}, \quad \text{(A8)}$$

and

$$S_2^{(0,4)}(x) = 0. \quad \text{(A9)}$$

Taking $x = \cos\bar{\theta}$ and inserting these results into Eq. (23) finally yields Eqs. (25)–(27) and (29).

APPENDIX B: FINITE SIZE CORRECTION δF_{11}

We present the line of reasoning leading to the formula for the correction δF_{11} to the free energy used in Fig. 3(a). The starting point is the assumption that this correction can be associated with the work $-\boldsymbol{f}_{\text{c.m.}}\cdot\boldsymbol{r}_{\text{c.m.}}$ done by the external body force $\boldsymbol{f}_{\text{c.m.}}$ in displacing the center of mass of the liquid by $-\boldsymbol{r}_{\text{c.m.}}$, where $\boldsymbol{r}_{\text{c.m.}}$ is the deviation of the position of the center of mass due to the nonvanishing volume of the immersed parts of the particles. For simplicity, we assume that the two particles lie in the xz plane and that their positions are given by the directions $\Omega_1 = (\bar{\theta}/2,0)$ and $\Omega_2 = (\bar{\theta}/2,\pi)$. In such a case and for spherical Janus particles composed of equal hemispheres one obtains approximately $\boldsymbol{r}_{\text{c.m.}} = [0,0,-(a^3/R_0^2)\cos(\bar{\theta}/2)]$. The body force $\boldsymbol{f}_{\text{c.m.}}$ counterbalances the net force acting on the center of mass due to the external torques acting on the particles. It follows from the spherical geometry that a capillary dipole Q_1 is associated with a net force on the droplet of magnitude $\delta f/(\gamma a) = Q_1 a/R_0$ in the direction determined by the orientation of the particle ϕ_i in the plane perpendicular to Ω_i. Accordingly one obtains $\boldsymbol{f}_{\text{c.m.}} = [0,0,2\delta f\sin(\bar{\theta}/2)]$ for the configuration $\leftarrow\rightarrow$, $\boldsymbol{f}_{\text{c.m.}} = (0,-2\delta f,0)$ for $\uparrow\ \uparrow$, and $\boldsymbol{f}_{\text{c.m.}} = 0$ for $\uparrow\ \downarrow$. This finally yields $\delta F_{11}/(\gamma a^2) = Q_1(a/R_0)^3\sin\bar{\theta}$ for $\leftarrow\rightarrow$ and $\delta F_{11} = 0$ for the remaining two configurations.

The above finite-size correction leads to a very good agreement between the analytical and numerical results and as such provides a useful semiempirical formula. However, our argumentation here does not amount to a strict derivation. Promoting the present line of reasoning toward a consistent overall finite size theory for all multipoles including monopoles and dipoles appears to be nontrivial in that the boundary condition for the contact line turns out to be relevant (our numerical calculations of F_{00} were performed for a free contact line and those of F_{11} for a pinned one). Extending this finite size theory is left for future research.

[1] K. Zahn and G. Maret, Phys. Rev. Lett. **85**, 3656 (2000).
[2] A. Domínguez, M. Oettel, and S. Dietrich, Phys. Rev. E **82**, 011402 (2010).
[3] B. Madivala, J. Fransaer, and J. Vermant, Langmuir **25**, 2718 (2009).
[4] P. A. Kralchevsky and K. Nagayama, Adv. Colloid Interface Sci. **85**, 145 (2000).
[5] M. Oettel, A. Domínguez, and S. Dietrich, Phys. Rev. E **71**, 051401 (2005).
[6] A. Domínguez, M. Oettel, and S. Dietrich, J. Chem. Phys. **128**, 114904 (2008).
[7] A. Würger, Europhys. Lett. **75**, 978 (2006).
[8] A. Domínguez, M. Oettel, and S. Dietrich, Europhys. Lett. **77**, 68002 (2007).
[9] J. Guzowski, M. Tasinkevych, and S. Dietrich, Eur. Phys. J. E **33**, 219 (2010).
[10] J. Guzowski, M. Tasinkevych, and S. Dietrich, Soft Matter **7**, 4189 (2011).
[11] A. Domínguez, in *Structure and Functional Properties of Colloidal Systems*, edited by R. Hidalgo-Àlvarez (CRC, Boca Raton, FL, 2010), p. 31.
[12] K. D. Danov and P. A. Kralchevsky, Adv. Colloid Interface Sci. **154**, 91 (2010).
[13] M. M. Nicolson, Proc. Cambridge Philos. Soc. **45**, 288 (1949).
[14] N. Aubry, and P. Singh, Phys. Rev. E **77**, 056302 (2008).
[15] J. Guzowski, PhD. thesis, University of Stuttgart (2010).
[16] R. Di Leonardo, F. Saglimbeni, and G. Ruocco, Phys. Rev. Lett. **100**, 106103 (2008).
[17] P. A. Kralchevsky, V. N. Paunov, I. B. Ivanov, and K. Nagayama, J. Colloid Interface Sci. **151**, 79 (1992).
[18] H. Lehle, E. Noruzifar, and M. Oettel, Eur. Phys. J. E **26**, 151 (2008).
[19] J. C. Loudet, A. M. Alsayed, J. Zhang, and A. G. Yodh, Phys. Rev. Lett. **94**, 018301 (2005).
[20] J. C. Loudet and B. Pouligny, Europhys. Lett. **85**, 28003 (2009).
[21] J. B. Fournier and P. Galatola, Phys. Rev. E **65**, 031601 (2002).
[22] D. Stamou, C. Duschl, and D. Johannsmann, Phys. Rev. E **62**, 5263 (2000).
[23] E. A. van Nierop, M. A. Stijnman, and S. Hilgenfeldt, Europhys. Lett. **72**, 671 (2005).
[24] H. Lehle and M. Oettel, Phys. Rev. E **75**, 011602 (2007).
[25] K. Brakke, Exp. Math. **1**, 141 (1992).

[26] Different from Eqs. (20)–(25) in Ref. [9], here we do not include the small parameter ϵ—introduced therein and associated with an external force—into the definition of the dimensionless quantities.

[27] D. C. Morse and T. A. Witten, Europhys. Lett. **22**, 549 (1993).

[28] The total force $f_{\text{c.m.}}$ in the z direction acting on a spherical droplet of volume V due to a constant body force density $\boldsymbol{f}_{\text{c.m.}}/V = (f_{\text{c.m.}}/V)\boldsymbol{e}_z = \text{const}$ can be written as $f_{\text{c.m.}} = (f_{\text{c.m.}}/V)\int_V dV = (f_{\text{c.m.}}/V)\oint_{\partial V} d^2s z\boldsymbol{n}\cdot\boldsymbol{e}_z = (f_{\text{c.m.}}/V)R_0^3\int d^2\Omega\cos\theta\boldsymbol{e}_r\cdot\boldsymbol{e}_z$, where $\boldsymbol{n}$ is the outward pointing normal of the interface which on a sphere equals $\boldsymbol{e}_r$. On the other hand, we can write $\boldsymbol{f}_{\text{c.m.}} = \int d^2s\pi_{\text{c.m.}}(\Omega)\boldsymbol{e}_r$ so that $\boldsymbol{f}_{\text{c.m.}}\cdot\boldsymbol{e}_z = f_{\text{c.m.}} = R_0^2\int d^2\Omega\pi_{\text{c.m.}}(\Omega)\boldsymbol{e}_r\cdot\boldsymbol{e}_z$. Accordingly, the effective pressure field reads $\pi_{\text{c.m.}}(\Omega) = 3f_{\text{c.m.}}\cos\theta/(4\pi R_0^2) = (f_{\text{c.m.}}/R_0^2)\sqrt{3/(4\pi)}Y_{10}(\Omega)$. The order l of spherical harmonics is not affected by rotations of the coordinate system (see, e.g., Ref. [29]) so that independently of choosing the z axis the pressure field $\pi_{\text{c.m.}}$ has only components with $l = 1$.

[29] D. M. Brink and G. R. Satchler, *Angular Momentum*, 2nd ed. (Clarendon, Oxford, 1968), p. 52.

[30] In our previous works (Refs. [9] and [10]) we have denoted $\tilde{\pi}$ simply as π.

[31] A. R. Edmonds, *Angular Momentum in Quantum Mechanics*, 2nd ed. (Princeton University Press, Princeton, 1957).

[32] A. P. Prudnikov, Y. A. Brychkov, and O. I. Marichev, *Integrals and Series*, 2nd ed. (Gordon and Breach, New York, 1986), Vol. 2.

[33] For details see the derivation of the analogous correction δF in the case of a hemispherical sessile droplet (Eq. (79) in Ref. [9]). In the case of a full droplet the free energy is twice as large and we have $\delta F_{00} = 2\delta F$. However, we note that this formula for δF_{00} holds only for $\theta_p = \pi/2$.

[34] Strictly speaking one should take (skipping indices) $Q_1 = \boldsymbol{T}\cdot\boldsymbol{\psi}/(|\boldsymbol{\psi}|\gamma a^2)$. This would make a difference in the case that the external torque $\boldsymbol{T}$ and the rotation vector $\boldsymbol{\psi}$ are not collinear. However, in our numerical calculations we always consider the case $\boldsymbol{T}\parallel\boldsymbol{\psi}$.

[35] In Figs. 2 and 3, for clarity, we show the numerical results from which the finite-size effects have been subtracted in order to facilitate comparison with the point-particle limit ΔF_{nn} for $n = 0,1$. It should be recalled that the actual free energy for particles of finite size contains these effects and reads $\Delta F = \Delta F_{nn} + \delta F_{nn}$, where $\delta F_{nn} \to 0$ for $a/R_0 \to 0$.

[36] S. Kim and S. J. Karilla, *Microhydrodynamics: Principles and Selected Applications* (Butterworth-Heinemann, New York, 1991).

[37] In the case $R_0/a \gg 1$ the hydrodynamic friction provides kinetic stability of the bubble at the time scale Δt associated with the rearrangement of the particles. This can be shown in terms of the following dimensional analysis. In the viscous regime the capillary force of the order γa leads to a tangential velocity of the particles of the order $\gamma a/(\eta a)$. Accordingly, the particles are brought into contact typically after the time $\Delta t = R_0\eta/\gamma$. On the other hand, the capillary force of the same order pushes together the inner and outer interfaces of the bubble. The corresponding friction in the liquid film according to lubrication theory [36] scales as $\eta R_0^2/H_0$, where $H_0 < 2a$ is the thickness of the film. Accordingly, the relative normal velocity of the interfaces scales as $\gamma a H_0/(\eta R_0^2)$ and the corresponding time scale $\Delta t_{\text{c.m.}}$ associated with the rearrangement of the center of mass of the bubble is $\Delta t_{\text{c.m.}} = R_0^2\eta/(\gamma a)$. The time scales Δt and $\Delta t_{\text{c.m.}}$ are well separated provided that $\Delta t_{\text{c.m.}}/\Delta t = R_0/a \gg 1$. In such a case during the time Δt the center of mass of the bubble is effectively fixed in space which is one of the requirements for our perturbation theory.

[38] W. Wang, R. Xie, X.-J. Ju, T. Luo, L. Liu, D. A. Weitz, and L.-Y. Chu, Lab Chip **11**, 1587 (2011).

[39] M. Abramowitz and I. A. Stegun, *Handbook of Mathematical Functions* (US Government Printing Office, Washington, DC, 1970).